ANOMALOUS CHLORINE IN IRON-RICH STRATA, YELLOWJACKET FORMATION, LEMHI COUNTY, IDAHO: ANALYTICAL DATA AND DISCUSSION

By

J.T. Nash, J.J. Connor, K.J. Curry, and C.S. Papp

Open-File Report 90-721

U.S. Geological Survey, DFC, Box 25046, MS 973, Denver, CO 80225

1990

CONTENTS

ILLUSTRATIONS

TABLES

ANOMALOUS CHLORINE IN IRON-RICH STRATA, YELLOWJACKET FORMATION, LEMHI COUNTY, IDAHO: ANALYTICAL DATA AND DISCUSSION

By

J.T. NASH, J.J. CONNOR, K.J. CURREY, and C.S. PAPP

ABSTRACT

Uncommonly high concentrations of chlorine, in the range of 0.1 to 1.10 wt percent, occur in samples collected from biotite-rich strata of the Middle Proterozoic Yellowjacket Formation. New analytical results for Cl and F in 539 samples are reported and briefly described. Although many of the biotite-rich samples having very high Cl are from Co-Cu-Au deposits of the Blackbird mining district, similar lithologies more than 10 km from ore deposits also are Cl-rich.

Chlorine correlates with biotite content, and locally with scapolite, with Fe and K, but not with F. Microprobe analyses have shown that Cl resides in the lattice of Fe-rich biotite. Chlorine appears to have been enriched early in the history of these rocks, but the mechanisms are not established. Unlike some metasedimentary rocks containing scapolite and high Cl, there is no evidence for evaporitic rocks in the Yellowjacket Formation that could have been a source of the Cl. More likely, the Cl reflects a stratified submarine brine that also carried Fe and K. Lithostratigraphic zones rich in Fe-K-Cl appear to be lateral equivalents of those hosting stratiform base-metal deposits. Rocks having anomalous Fe-K-Cl are considered to be a guide to sub-basins favorable for stratiform base-metal deposits.

INTRODUCTION

Uncommonly high concentrations of chlorine were observed in biotite grains and in a limited suite of metasedimentary rock samples in and near the Blackbird mine (Nash, 1989A). This report provides new results of analyses of Cl and F in 539 rock samples. It is now clear that anomalous concentrations of Cl occur in strata long distances from known copper-cobalt ore deposits and are not directly related in a simple manner to ore-forming fluids. Although the geochemical mechanisms remain uncertain, high Cl concentrations are diagnostic of metalliferous stratigraphic zones or sub-basins in the Yellowjacket Formation and appear to reflect sedimentary and diagenetic processes that were favorable for concentrating base metals.

The main focus of this study is the occurrence of Cl in very dark, biotite-rich strata called "mafic volcaniclastic rocks" by Nash and Hahn (1989) and "biotitite" by Connor (1990). All samples having high to very high concentrations of Cl (>0.1 wt %) contain more than 50 percent biotite or biotite plus scapolite. Mafic dikes altered and metamorphosed to biotite-rich granofels also commonly contain elevated Cl concentrations. The layered biotite-rich rocks clearly originated as sediments and are interbedded at millimeter-to-meter scales with typical Yellowjacket Formation argillite, siltite, and quartzite. Scapolite porphyroblasts are prominently confined to compositional layers. Biotite in the mafic strata tends to be coarser than in nearby argillites, has high luster, and rarely is oriented. Carbonate strata are notably absent, except in one small part of the area in which an impure marble lens occurs in the lower unit of the Yellowjacket Formation. Carbonate minerals in veins or as cement are also very rare, except in altered dikes of the Blackbird mine area. Iron-rich strata are important in the area as hosts for copper-cobalt deposits (Nash and Hahn, 1989). During geochemical studies of those lithologies throughout the region, we found that most of the Fe-silicate (biotite) variety also are characterized by very unusual amounts of Cl.

GEOLOGIC SETTING

An enormously thick (>13,000 m) section of fine-grained Proterozoic siliciclastic rocks occurs in the Salmon River Mountains in the vicinity of the Blackbird mine (Connor, 1990). These rocks are broadly folded and locally faulted, but the thickness of the section does not appear to be caused by structural repetition. Most of the Proterozoic metasedimentary rocks are assigned to the Yellowjacket Formation (Ross, 1934; Lopez, 1981; Hughes, 1983; Connor and Evans, 1986; Connor, 1990). The Yellowjacket Formation in the Idaho Cobalt Belt comprises metamorphosed (biotite-grade), generally dark-colored, fine-grained and thinly-bedded to laminated impure argillite, siltite, quartzite, and minor marble. Dark colors generally distinguish the Yellowjacket Formation from other Proterozoic units.

The area underwent at least one period of metamorphism and deformation in the Proterozoic, and rocks of the region were thrust eastward during Paleozoic(?) and Cretaceous orogenies, and later cut by Cenozoic normal faults. Regional greenschist metamorphism occurred prior to contact metamorphism associated with 1,370 Ma granitic plutons (Evans and Zartman, 1990).

The Yellowjacket Formation in east-central Idaho is the oldest sedimentary unit in a Proterozoic section that is more than 13,000-m thick. Regionally, and in the mine area, three lithostratigraphic units can be distinguished (Hughes, 1983; Connor, 1990) (fig. 1). The lower unit, more than 5,000-m thick, is very fine-grained and characteristically has interlaminated to thinly interbedded grey-green argillite and siltite with lesser amounts of fine-grained quartzite. Sedimentary features were interpreted by Hughes (1983) as indicating deposition in a deep marine basin by turbidity currents, although other features such as mud cracks suggest shallow-water environments. Impure, scapolite-bearing marble strata occur locally. A stratigraphic zone, roughly following the top of the lower unit, contains visible fine-grained magnetite and pyrite laminae (Connor, 1990). At a few localities near Iron Creek, magnetite or pyrite comprises more than 50 percent of beds that are a few centimeters to 3-m thick (Nash, 1989B). The upper part of the lower unit is magnetic and is prominent in regional airborne magnetic surveys (Connor, 1990).

The middle unit, of variable thickness but up to 5,000 m in the area of the Idaho Cobalt Belt, generally contains plane parallel, laminated to thin-bedded siltite-argillite couplets that produce a prominent black and white banding in outcrops. The middle unit is a complex of coarsening upward cycles of argillite, siltite, and fine-grained quartzite, and contains distinctive interbeds of biotite-rich rock. Zircon from mafic beds in the middle unit yielded apparent U-Pb ages of about 1,670-1,700 Ma (Hahn and

Hughes, 1984); these ages should be considered maximum ages because of possible inherited radiogenic lead (K.V. Evans, written commun., 1986). Sedimentary structures are abundant in this unit and include graded beds, silt-sand couplets, flute casts, load structures, slumped beds, and sand dikelets. According to Hughes (1983), these clastic sediments were deposited in a submarine fan complex, but other interpretations are possible.

A stratigraphic zone near the top of the middle unit contains strata rich in black biotite (Hahn and Hughes, 1984; Nash and Hahn, 1989; Connor, 1990) (fig. 2). Most of the strata having anomalous chlorine are "biotitite" (mafic beds) from this zone. Individual mafic beds are 1 cm to more than a meter thick. The mafic strata are most abundant and thickest in the ore zones of the Blackbird mine area (Nash and Hahn, 1989) but are also well developed and exposed in Deep Creek Canyon 10-15 km east of the mine. The continuity of individual mafic beds can not be determined in outcrop, but can be correlated between drillholes 100-m apart. Mafic beds tend to be massive or faintly laminated and generally are not foliated. Depending upon metamorphic grade they are comprised chiefly of biotite or biotite-garnet ± chloritoid, and strata outside of the mine area commonly contain 5-30 percent scapolite porphyroblasts. Biotite-rich argillites resemble mafic rocks but have finer-grained metamorphic biotite, more clastic quartz grains and layers, and graded bedding; argillites invariably contain low concentrations of chlorine (<0.1 wt %).

The upper unit of the Yellowjacket Formation in the area is as much as 3,000-m thick and is mostly thin- to thick-bedded very-fine to fine-grained quartzite having planar laminations, and local ripple marks or hummocky cross-stratification (Connor, 1990). Interbeds of fine clastic rocks and mafic strata are rare.

Metamorphosed mafic dikes and sills 1- to 30-m thick intrude the Yellowjacket Formation. Although these rocks rarely crop out, they are common in float, drillcore, and mine workings. Mafic strata of the middle unit are most abundant in areas having mafic dikes and are chemically similar to the mafic dikes (Nash and Hahn, 1989).

Proterozoic granitic rocks intrude the Yellowjacket Formation about 3 km north and east of the Blackbird mine (fig. 1). The granitic rocks generally have large K-feldspar phenocrysts and some have gneissic fabric. Samples from various phases of the granitic pluton yield discordant Rb/Sr model ages of about 1,500 Ma (Armstrong, 1975) and zircons yield a more reliable U-Th-Pb age of 1,370 Ma (Evans and Zartman, 1990). Metamorphic grade increases toward the intrusive body, reaching a maximum grade of hornblende-cordierite-sillimanite in the contact zone.

Tertiary volcanic rocks of the Challis volcanic field are widespread north and east of the Blackbird mine. Tertiary mafic and felsic dikes fill some fault zones and intrude the Yellowjacket Formation in the mine.

The Fe-Cl-rich rocks that are the focus of this study are important as host rocks for cobalt deposits in the Idaho Cobalt Belt. Three types of Co-Cu deposits are recognized in the Idaho Cobalt Belt (Nash and Hahn, 1989) (fig. 1). (1) The most important of these are Co-Cu-As-rich deposits of Blackbird mine type, which contain approximately equal amounts of cobalt and copper minerals, generally cobaltite (CoAsS) and chalcopyrite, with variable amounts of gold and pyrite. The deposits have tabular form and are closely associated with mafic sequences in the upper part of the middle unit. (2) Cobaltiferous-pyrite deposits, with variable chalcopyrite content, occur in the lower unit of the Yellowjacket Formation at Iron Creek (Nash, 1989B), about 28 km southeast of the Blackbird mine (fig. 1). These deposits contain abundant very fine to coarse-grained pyrite. Bedded magnetite occurs below the Co-pyrite zones. (3) Cobaltite-bearing, tourmaline-cemented breccias are common in the lower, middle, and upper units of the Yellowjacket Formation for many kilometers south and east of the Blackbird mine. Only a few contain more than 0.1 percent Co.

GEOCHEMICAL STUDIES

Previous Studies

The 539 samples for this study were collected as part of geological and geochemical studies of the Idaho Cobalt Belt (Nash and Hahn, 1989; Connor, 1990). Most of the 372 samples studied by Nash were splits of drill core 5- to 40-cm long, and generally very fresh, unweathered rocks. The drill core samples have identification numbers typical of drill core, such as M4B-495, that indicate hole number and depth in feet. Samples from outcrops were collected for comparison with rocks in core; those outcrop samples have a prefix "NIC" (for Nash Idaho Cobalt). As part of regional mapping and geochemical studies, Connor collected a series of outcrop samples that were estimated to be typical of exposures south and east of the mine. The Connor samples (JCY series, table 2) are as fresh as possible from outcrop or float (generally only slightly weathered), and are thought to be an unbiased estimate of various litho-stratigraphic units. The rock samples were analyzed by standard methods of the U.S. Geological Survey (Baedecker, 1987), and most were examined in thin sections. Analytical results for major and minor elements in samples described here have been reported previously (Nash and others, 1988; Connor, 1990). Locations of the deposits sampled by Nash are shown on figure 1, and the locations of samples collected by Connor are given in table 2.

ANALYTICAL METHODS

Chloride and fluoride were determined by ion sensitive electrode (ISE) using methods described by Jackson and others (1987) and by Hopkins (1977), respectively. Chloride was determined after decomposition of the rocks with a mixture of sulfuric acid, hydrofluoric acid, and potassium permanganate in a Conway diffusion cell. Chlorine is subsequently distilled from the outer chamber and reduced to chloride in the inner chamber, which contains sodium sulfite and potassium hydroxide. The chloride in the inner chamber is measured directly with a chloride-sensitive ISE. Rock samples for fluoride analysis were fused with a sodium carbonate-potassium carbonate-potassium nitrate flux, then dissolved with citric acid. Sodium citrate is added to adjust ionic strength and to mask interferences from Al and Fe. Fluorine is determined in the citrate-buffered solution by ISE.

The lower limit of determination by these methods for a 0.2 g sample is 0.01 wt percent (100 ppm), which is appropriate for the range of concentrations found in these samples and our interest in concentrations greater than about 0.1 wt percent. Examination of results for different samples from closely spaced localities (table 2, samples from same outcrop with suffixes T, R, X) indicates that halogen concentrations are consistent for a lithology and reproducible by the laboratory.

New Results for Cl and F

The analytical results are reported in two tables to emphasize that the samples were collected independently and for different purposes. Data in table 1 are for samples collected by Nash as part of an intensive geochemical study focused primarily on the origin and evolution of the Cu-Co-Au ores of the Blackbird district. Data in table 2 are for samples collected by Connor in the period 1983-1985 as part of a regional geochemical examination of the Yellowjacket Formation.

Analytical results for 372 samples from the Blackbird mine area are in table 1. Included in table 1 are values for total iron, reported as Fe_2O_3, and potassium, reported as K_2O. Most of those values are from X-ray fluorescence (XRF) analysis as reported in Nash and others (1988), but for some samples with high As or Fe contents that could not be analyzed by XRF, values from induction coupled plasma (ICP) analysis are shown for completeness. Results for 124 samples collected by Connor are shown in table 2. As for table 1, results shown for Fe_2O_3 and K_2O determined by XRF. The information on iron and potassium are included to provide a geochemical description of the sample; possible discrepancies between XRF and ICP results should not be of sufficient magnitude to be significant in the characterization of the samples.

DISCUSSION

Concentrations and Distribution of Chlorine

These new halogen analyses confirm and extend the previous report (Nash, 1989A) of anomalous Cl in the Yellowjacket Formation. High concentrations of Cl, greater than about 0.1 wt percent, occur in many of our samples. Histograms for Cl and F in 124 representative samples collected by Connor indicate that most typical Yellowjacket samples contain less than about 0.05 wt percent Cl and less than 0.05 wt percent F (fig. 3). The histogram for Cl (fig. 3) suggests a possible trimodal distribution: (1) samples with less than 0.01 wt percent Cl, chiefly samples from the lower and middle unit; (2) samples with about 0.02 wt percent Cl, from all three units; and (3) anomalous samples with more than about 0.07 wt percent Cl, chiefly siltite from the upper unit and biotitite. Connor's biotitite samples contain 0.12 to 0.81 wt percent Cl. Concentrations of Cl in excess of 0.1 percent are rare in rocks (Fuge, 1978; Guidotti, 1984). Analytical data for more than 500 samples suggest that F and Cl concentrations are not correlated (fig. 4), and that the amount of F in our samples is within the normal range (Koritnig, 1978). Subsequent discussion will focus on only Cl.

Numerous samples from the Blackbird ore deposits contain 0.5 to 1.1 wt percent Cl, but stratigraphically equivalent rocks also contain highly anomalous (0.1-0.8 wt %) Cl far beyond known mineralization. We can not document the full extent of the anomaly, because of structural displacement of key units, the presence of a large intrusive body, and lack of outcrop. The Cl anomaly may have once been continuous from the Blackbird mine for more than 15 km to the east through Deep Creek canyon (fig. 2).

There is a strong bulk compositional control on the occurrence of high Cl values. Chlorine correlates strongly with Fe and K (figs. 5 and 6). The high Fe, K, and Cl occur together in biotite (Nash, 1989A), the chief site for Cl in these rocks. Scapolite possibly carries substantial amounts of Cl in some strata, but this has not yet been confirmed by microprobe analysis. Rocks with normal amounts of Fe and K, as in typical Yellowjacket Formation argillites and siltites, do not contain much Cl. There is no correlation of Cl with Na, and many rocks have much less Na than Cl, thus halite is not a major factor in the Cl geochemistry of the metasedimentary rocks.

Low Cl concentrations (<0.1 wt %) in many samples are possibly ambiguous regarding the presence of Cl at those localities. The compositional control discussed above, can be interpreted to mean that high Cl values are *retained* only in biotite or biotite-scapolite strata because of the ability of those phases to host Cl. If this hypothesis is correct, then the low Cl values do not necessarily indicate low Cl fluids.

The cycle of Cl in these rocks, discussed by Nash (1989A), still is not clear. The new results for Cl confirm the bulk chemical and mineralogical associations noted by Nash, but do not provide an unequivocal answer to the source and timing of Cl introduction. The stratiform geometry of the high Cl rocks, along with Fe and K, seems to be evidence for a sedimentary mode of occurrence of these elements as chemical sediments, or perhaps a reflection of sedimentary permeability for flow of diagenetic pore fluids. However, mafic dikes and sills also are rich in K and Cl, and the enrichment in those rocks must be post-sedimentation by metasomatic processes. Of course, K and Cl could have moved at several times in the complex history of these rocks. If K and Cl were introduced at one time, that most likely was during diagenesis (assuming that mafic dikes and sills were emplaced shortly after sedimentation, as proposed by Hahn and Hughes (1984) and Nash and Hahn (1989). The universal absence of fractures filled with biotite implies that the K-Cl metasomatism occurred in partly consolidated sediments.

The basis for the Fe-Cl association is not clear. One reason may be that Cl-rich fluids transported the Fe (Barnes, 1979). However, Cl is *not* enriched in Fe-rich, magnetite- or pyrite-bearing argillite and cobaltiferous-pyrite lenses of the lower unit in the Iron Creek area. However, biotite is not well developed in those rocks and there may have been no phase to retain Cl.

Source of Chlorine: Evaporites or Brine?

The stratiform character and wide lateral extent of rocks having anomalous Fe-K-Cl is suggestive of sedimentary processes and possibly a relation to evaporites. However, the stratigraphy and bulk composition of these Cl-rich rocks differ significantly from many classic scapolitic occurrences that have been interpreted to be meta-evaporites (Heitanen, 1967; Serdyuchenko, 1975; Ramsay and Davidson, 1970). The Cl-rich Yellowjacket strata are rich in Fe rather than Ca-Mg, and there are no associated carbonate strata or carbonate mineral cements. Calcium and magnesium in these rocks reside almost entirely in silicate minerals. The lack of evidence for Ca-Mg carbonate or sulfate strata argues strongly against conventional evaporite sedimentation (Schreiber, 1986) in exposed parts of the Yellowjacket Formation.

There are two possible scenarios, unlikely in our opinion, that might explain the lack of supporting evidence for evaporites in the Yellowjacket Formation. One explanation could be obliteration of cogent evidence by alteration, which can be a major problem in the study of evaporites (Schreiber, 1986). However, we feel that some evidence for carbonates, sulfates, and desiccation features should have been preserved and sufficiently visible for us to have detected them. A second possibility is that the evaporitic part of the Yellowjacket comprised such a minor part of the sequence that it yielded only small quantities of evaporitic rocks. The mass balances of evaporite deposition from sea water indicate that the ratio of NaCl (halite) to $CaSO_4$ (gypsum or anhydrite) is about 22:1 by volume from a closed system (Hardie, 1984), which indicates that halite can predominate over gypsum under unusual conditions. Ratios of 3:1 to as low as 1:100 in natural evaporites are caused by reflux, addition of meteoric groundwater, and alteration (Schreiber, 1986). *If* there was a closed system in a Yellowjacket sub-basin, presumably of short duration, evaporite deposition *might* have yielded extremely thin beds in which halite exceeded gypsum or anhydrite. Calculations by Mora and Valley (1989) indicate that Cl-rich biotite-scapolite rocks similar to those in the Yellowjacket can evolve from sedimentary layers having only 10 modal percent halite.

The geometry and composition of the anomalous Yellowjacket strata are possibly more consistent with formation from submarine or diagenetic brines (Nash, 1989A). Brines in Modern submarine hydrothermal systems have salinities as high as about 26 wt percent and temperatures in the range of 50 to >300 °C and carry very high concentrations of base metals (Degans and Ross, 1969; Von Damn and Bischoff, 1987). The Red Sea brines are stratified, which by analogy could help explain the lateral extent of the Yellowjacket anomaly. Hot, saline brines that develop as sedimentary pore fluids in the Salton Sea geothermal field or oil fields (Helgeson, 1968; Hanor, 1979) are other possible analogs. Structural features in the Yellowjacket Formation have been interpreted as resulting from upward movement of pore fluids during periods of overpressure (Nash and Hahn, 1989; Nash, 1989). These pore fluids probably vented to the seafloor at sites of slumping and soft-sediment disruption.

The postulated brine has important implications for metal transport and mineral deposit morphology. The brine would have been capable of transporting significant amounts of iron as well as base metals if fo_2 and fs_2 were low (Lydon, 1983). The high Cl concentrations possibly explain the geometry of the iron silicate facies and the occurrence of the large Cu-Co ore deposits in them. Numerical modelling and observations of modern seafloor geothermal systems demonstrate the role of salinity, along with temperature, in controlling the flow of submarine brines (Lydon, 1983; Zierenberg, 1990). Brines with density lower than seawater are buoyant and tend to form small (but rich) mineral deposits, whereas some rare highly saline, hydrothermal brines are more dense than seawater and can become stratified in submarine basins and form laterally extensive mineral deposits.

The residence of Cl in these strata prior to metamorphism remains an unsolved problem. We have seen no textures suggestive of evaporite minerals (such as halite casts), as are known in the Wallace and Missoula Formations of the Belt Supergroup in northern Idaho and Montana (Heitanen, 1967; Grotzinger, 1986). We have found no references to diagenetic or very low grade metamorphic silicate minerals that contain substantial amounts of Cl. For instance, chlorite and smectite do not appear to incorporate Cl.

SUMMARY

High concentrations of Cl are found in Yellowjacket Formation strata that are rich in Fe and K. Fluorine concentrations are normal and do not correlate with Cl. Highest and most consistent Cl concentrations occur in the area of the Blackbird mine where mafic volcaniclastic strata are most abundant, but similar Cl concentrations occur in Fe-K-rich strata more than 10 km from known mineral deposits. The stratiform character of the anomalous rocks suggests they formed as chemical sediments, possibly modified during diagenesis, and were preserved by isochemical metamorphism. The composition of these Cl-rich strata is distinctly higher in Fe and K, and lower in Ca and Mg than postulated meta-evaporites elsewhere, and evidence for associated evaporites in the Yellowjacket is lacking. Most likely the Fe, K, and Cl were carried by a hydrothermal brine on or near the seafloor. Density stratification similar to that in the Modern Red Sea would have caused the postulated brine to flow laterally from seafloor vents to fill a sedimentary sub-basin tens of kilometers wide. The Fe-K-Cl-rich strata appear to be lateral equivalents to those containing base metals at the Blackbird mine.

REFERENCES CITED

Armstrong, R.L., 1975, Precambrian (1,500 m.y. old) rocks of central Idaho--the Salmon River Arch and its role in Cordilleran sedimentation and tectonics: American Journal of Science, v. 275-A, p. 437-467.

Baedecker, P.A., (ed), 1987, Methods for Geochemical Analysis: U.S. Geological Survey Bulletin 1770, p. IN1-K5.

Barnes, H.L., 1979, Solubilities of ore minerals, *in* Barnes, H.L., ed., Geochemistry of Hydrothermal Ore Deposits, Second Edition: New York, John Wiley, p. 404-460.

Braitsch, O., 1971, Salt Deposits--Their Origin and Composition: Berlin, Springer-Verlag, 297 p.

Connor, J.J., 1990, Geochemical stratigraphy of the Yellowjacket Formation (Middle Proterozoic) in the area of the Idaho Cobalt Belt, Lemhi County, Idaho, Part A. Discussion; Part B., Geochemical Data: U.S. Geological Survey Open-File Report 90-0234 A and 90-0234B, 40 p.

Connor, J.J., and Evans, K.V., 1986, Geologic map of the Leesburg quadrangle, Lemhi County, Idaho: U.S. Geological Survey Map MF-1880 (scale 1:62,500).

Degens, E.T., and Ross, D.A., 1969, Hot Brines and Recent Heavy Metal Deposits in the Red Sea: New York, Springer-Verlag, 600 p.

Evans, K.V., and Zartman, R.E., 1990, U-Th-Pb and Rb-Sr geochronology of middle Proterozoic granite and augen gneiss, Salmon River Mountains, east central Idaho: Geological Society of America Bulletin, v. 102, p. 63-73.

Fuge, R., 1978, Chlorine, parts B-O, *in* Wedepohl, K.H., ed., Handbook of Geochemistry: New York, Springer-Verlag, p. 17B-17O.

Grotzinger, J.P., 1986, Shallowing-upward cycles of the Wallace Formation, Belt Supergroup, northwestern Montana and northern Idaho: Montana Bureau Of Mines and Geology, Special Publication 94, p. 143-160.
Guidotti, C.V., 1984, Mica in metamorphic rocks, *in* S.W. Bailey, ed., Micas: Mineralogical Society of America, Reviews in Mineralogy, v. 13, p. 357-468.
Hahn, G.A., and Hughes, G.J., Jr., 1984, Sedimentation, tectonism, and associated magmatism of the Yellowjacket Formation in the Idaho Cobalt Belt, Lemhi County, Idaho, in Hobbs, S.W., ed., The Belt, Abstracts with Summaries, Belt Symposium II, 1983: Montana Bureau of Mines and Geology, Special Publication 90, p. 65-67.
Hanor, J.S., 1979, The sedimentary genesis of hydrothermal fluids, *in* Barnes, H.L., ed., Geochemistry of Hydrothermal Ore Deposits (Second Edition): New York, Wiley-Interscience, p. 137-172.
Hardie, L.A., 1984, Evaporites: marine or non-marine: American Journal of Science, v. 284, p. 193-240.
Heitanen, A.H, 1967, Scapolite in the Belt Series in the St. Joe-Clearwater region, Idaho: Geological Society of America, Special Paper 86, 56 p.
Helgeson, H.C., 1968, Geologic and thermodynamic characteristics of the Salton Sea Geothermal System, American Journal of Science, v. 266, p. 129-166.
Hopkins, D.M., 1977, An improved ion-sensitive electrode method for the rapid determination of fluorine in rocks and soils: Journal of Research of U.S. Geological Survey, v. 5, p. 589-593.
Hughes, G.J., Jr., 1983, Basinal setting of the Idaho Cobalt Belt, Blackbird mining district, Lemhi County, Idaho; in The Genesis of Rocky Mountain Ore Deposits--Changes with Time and Tectonics: Denver Region Exploration Geologists Society, p. 21-27.
Jackson, L.L., Brown, F.W., and Neil, S.T., 1987, Major and minor elements requiring individual determinations, classical whole rock analysis and rapid rock analysis, *in* Baedecker, ed., Methods for geochemical analysis: U.S. Geological Survey Bulletin 1770, p. G1-G23.
James, H.L., 1954, Sedimentary facies of iron-formation: Economic Geology, v. 49, p. 235-293.
Koritnig, S., 1978, Fluorine, parts B-O, *in* Wedepohl. K.E., ed., Handbook of Geochemistry: New York, Springer-Verlag, p. 9B-9O.
Lopez, D.A., 1981, Stratigraphy of the Yellowjacket Formation of east-central Idaho: U.S. Geological Survey Open-File Report 81-1088, 203 p.
Lydon, J.W., 1983, Chemical parameters controlling the origin and deposition of sediment-hosted stratiform lead-zinc deposits, *in* Sangster, D.F., ed., Sediment-hosted Stratiform Lead-Zinc Deposits: Mineralogical Association of Canada, Short course handbook 8, p. 175-250.
Mora, C.I., and Valley, J.W., 1989, Halogen-rich scapolite and biotite: Implications for metamorphic fluid-rock interaction: American Mineralogist, v. 74, p. 721-737.
Nash, J.T., 1989A, Clorine-rich biotites from the Blackbird mining district, Lemhi County, Idaho--evidence for a saline hydrothermal brine: U.S. Geological Survey Open-File Report 89-445, 25 p.
Nash, J.T., 1989B, Geology and geochemistry of synsedimentary cobaltiferous pyrite deposits, Iron Creek, Lemhi County, Idaho: U.S. Geological Survey Bulletin 1882, 33 p.

Nash, J.T., and Hahn, G.A., 1989, Stratabound Co-Cu deposits and mafic volcaniclastic rocks in the Blackbird Mining district, Lemhi County, Idaho, *in* Boyle, R.W. and others, eds, Sediment-hosted Stratiform Copper Deposits: Geological Association of Canada, Special Paper 36, p. 339-356.

Nash, J.T., Briggs, Paul, Bartel, Ardith J., and Brandt, E.L., 1988, Analytical results for samples of ore and altered hostrocks, Blackbird mining district, Lemhi County, Idaho: U.S. Geological Survey Open-File Report 88-661, 71 p.

Ramsay, C.R., and Davidson, L.R., 1970, The origin of scapolite in the regionally metamorphosed rocks of Mary Kathleen, Queensland, Australia: Contributions to Mineralogy and Petrology, v. 25, p. 41-51.

Ross, C.P., 1934, Geology and ore deposits of the Casto quadrangle, Idaho: U.S. Geological Survey Bulletin 54, 135 p.

Schreiber, B.C., 1986, Arid shorelines and evaporites, *in* Sedimentary Environments and Facies (Second Edition), Reading, H.G., ed.: London, Blackwell Scientific Publications, p. 189-228.

Serdyuchenko, D.P., 1975, Some Precambrian scapolite-bearing rocks evolved from evaporites: Lithos, v. 8, p. 1-7.

Von Damn, K.L., and Bischoff, J.L., 1987, Chemistry of hydrothermal solutions from the souther San Juan de Fuca Ridge: Journal of Geophysical Research, v. 92, no. B11, p. 11,328-11,342.

Zierenberg, R.A., 1990, Deposition of metalliferous sediment beneath a brine pool in the Atlantis II Deep, Red Sea, *in* G.R. McMurray, ed., Gorda Ridge, A seafloor Spreading Center in the United States' Exclusive Economic Zone: New York, Springer-Verlag, p. 131-142.

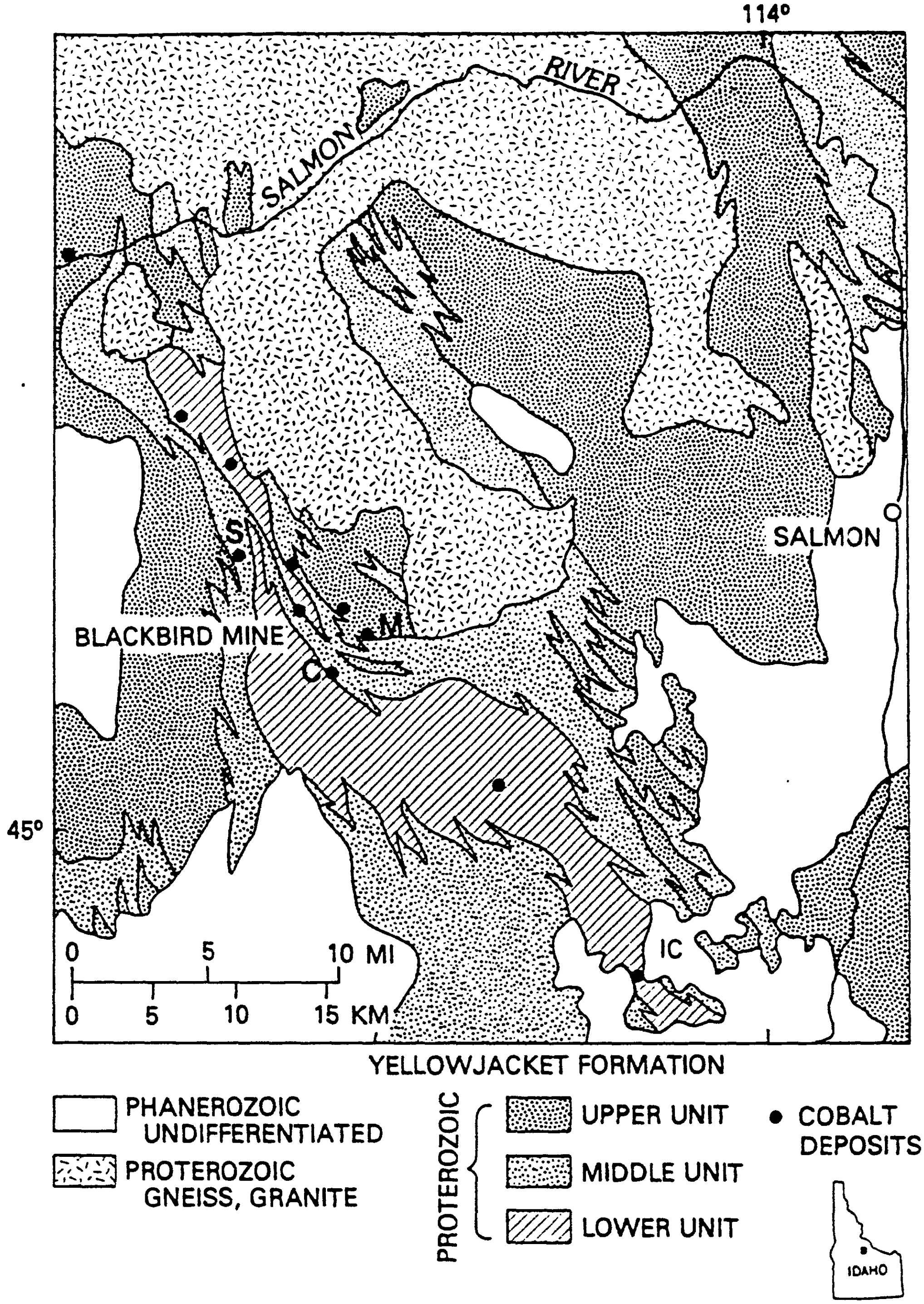

Figure 1. Location and generalized geology of the Idaho Cobalt Belt, Lemhi County, Idaho. Cobalt deposits sampled in this study: C, Conicu; IC, Iron Creek; M, Merle; S, Sunshine

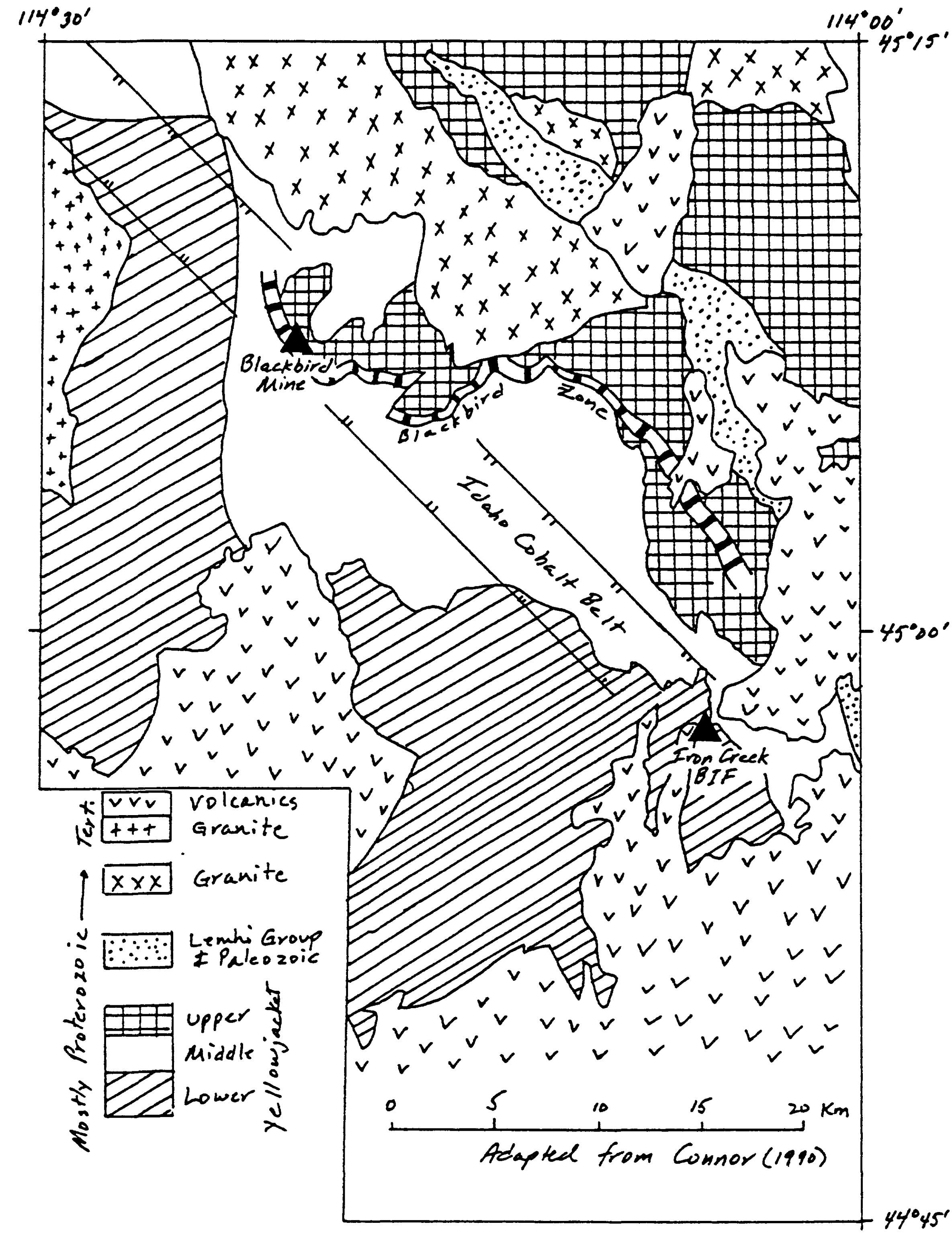

Figure 2. Geology of the Idaho Cobalt Belt, including the Blackbird stratigraphic zone that is the locus of most Cl-rich samples.

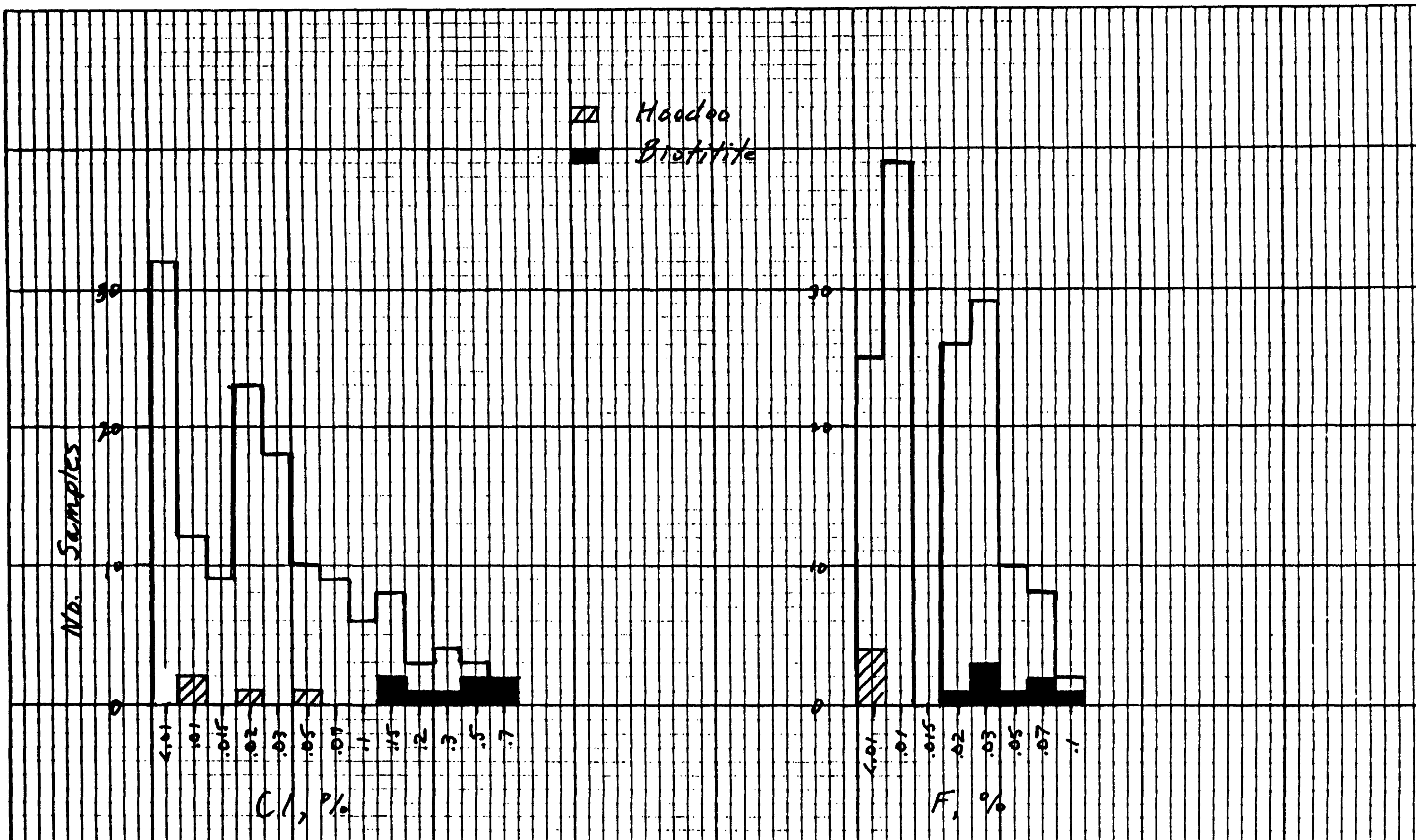

Figure 3. Histograms of Cl and F in Yellowjacket Formation samples.
A. Histogram of Cl. B. Histogram of F.

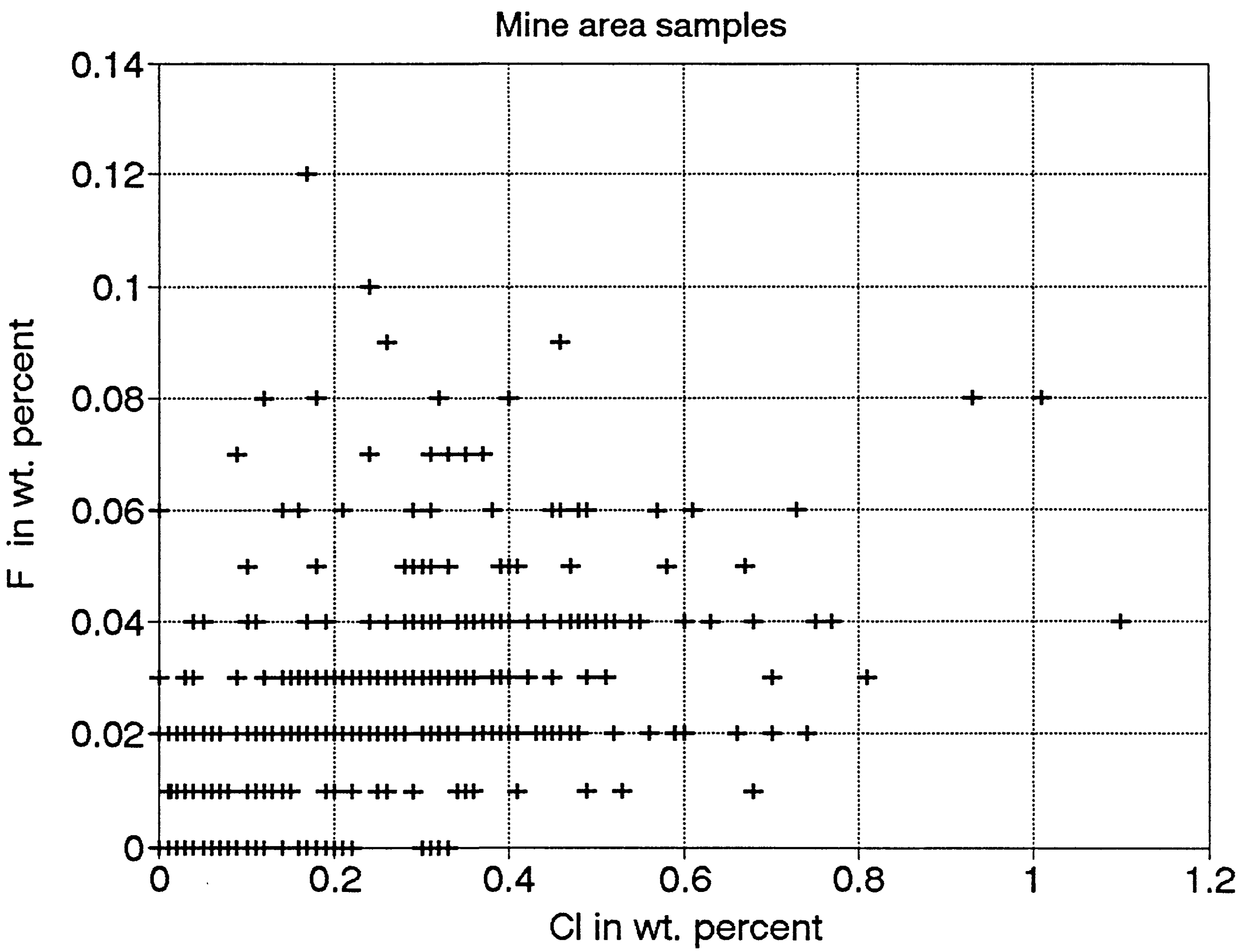

Figure 4. Plot of Cl vs F in samples from the Blackbird mine area. The correlation coefficient is 0.32, but the high degree of scatter suggests that the two elements behave independently.

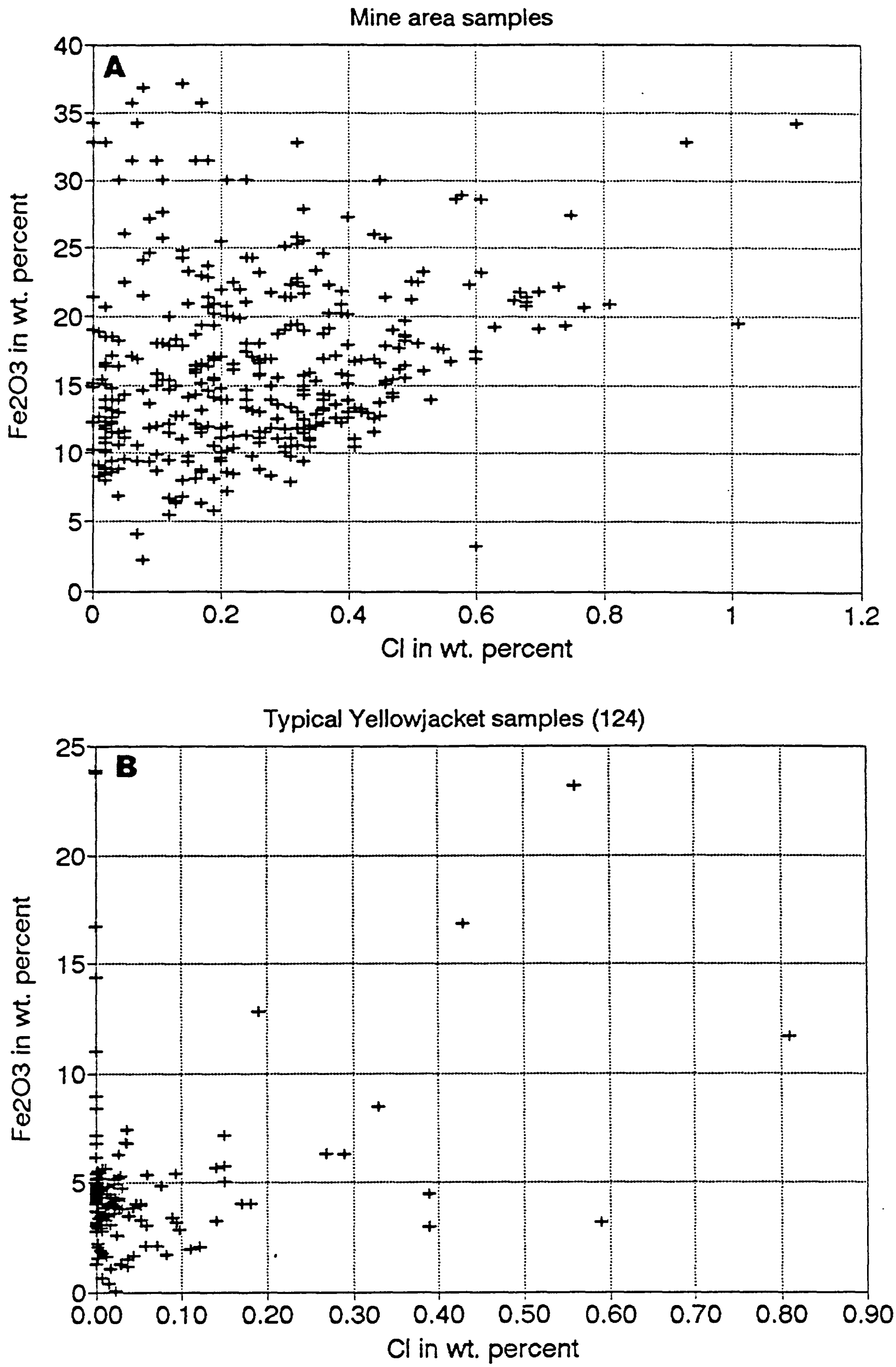

Figure 5. Plot of Cl vs Fe_2O_3. (A) Samples from the Blackbird mine area. The correlation coefficient for all samples (313 valid pairs) is 0.20, but for samples with more than 0.1 wt percent Cl there is a stronger correlation with Fe; (B) Typical samples distant from ore deposits. The correlation coefficient is 0.58, and the correlation is highest for samples containing more than about 0.1 wt percent Cl.

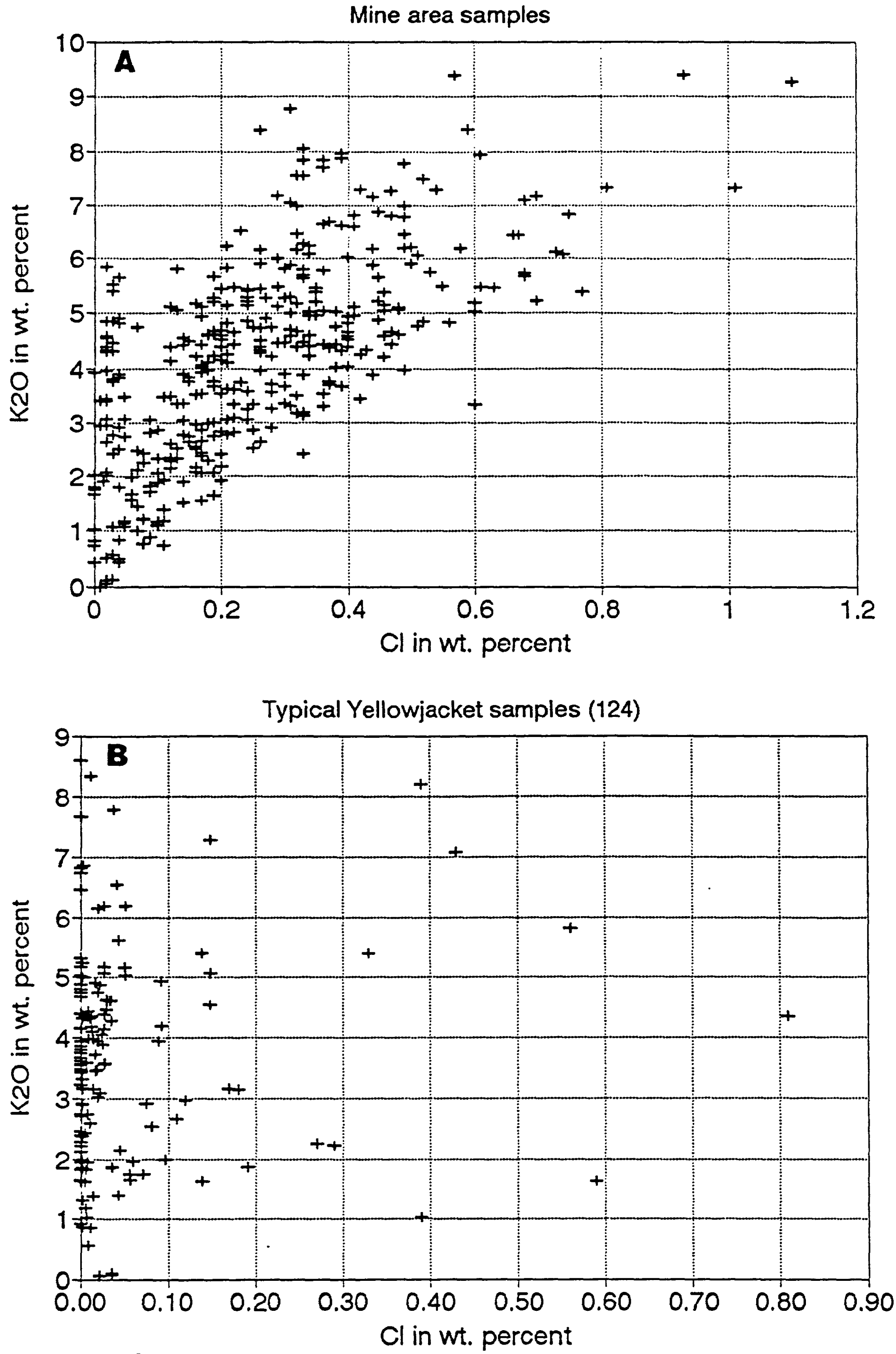

Figure 6. Plot of Cl vs K_2O. (A) Samples from the Blackbird mine area. The correlation coefficient is 0.66 for all samples (361 valid pairs), and the correlation is stronger for samples having more than about 0.1 wt percent Cl; (B) Typical samples distant from ore deposits. The correlation coefficient is 0.10, but there is a positive association in samples having more than 0.1 wt percent Cl.

Table 1. Analytical results for samples from within or near ore deposits of Idaho Cobalt Belt

[Fe_2O_3*, total iron determined by XRF or ICP, reported as Fe_2O_3; K_2O*, determined by XRF or ICP;
<, less than value shown; --, not analyzed]

Field no.	Fe_2O_3* %	K_2O* %	Cl %	F %	Lithol
Samples from drill core					
Conicu deposit					
C2A-0298	6.79	4.42	0.14	0.02	3
C2A-0310	8.16	5.18	0.16	0.03	3
C2A-0320	10.20	5.85	0.21	0.03	3
C2A-0341	8.61	5.13	0.17	0.03	3
C2A-0362	10.10	5.45	0.20	0.03	3
C3B-0289	10.40	5.49	0.22	0.03	3
C3B-0300	6.73	5.13	0.12	0.01	3
C3B-0410	8.57	0.56	0.03	0.02	3
C5A-0047	11.70	5.44	0.26	0.01	3
C5A-0283	13.70	2.83	0.09	0.07	9
Horseshoe deposit					
HO2A-610	19.10	4.45	0.47	0.02	5
HO2A-615	18.10	4.76	0.51	0.04	3
HO3A-383	28.60	9.40	0.57	0.06	5
HO3A-413	22.80	4.39	0.32	0.03	5
Iron Creek deposit					
IC3-064	9.16	3.42	0.01	0.02	2
IC3-072	14.90	1.04	<0.01	0.03	2
IC3-083	12.70	3.76	0.03	0.02	2
IC3-102	13.90	4.82	0.04	0.01	2
IC10-440	14.00	5.52	0.03	<0.01	2
IC10-806	16.40	4.91	0.04	0.02	2
IC10-807	16.40	3.91	0.04	0.02	2
IC10-809	80.08	0.72	<0.01	0.02	2
IC10-819	40.04	2.41	0.03	0.01	2
IC10-824	26.10	3.50	0.05	0.01	2
IC10-829	9.62	2.75	0.05	<0.01	2
IC12-265	12.40	4.32	0.03	<0.01	3
IC12-280	14.00	4.32	0.02	0.02	2
IC12-295	32.89	2.65	0.02	<0.01	2
IC12-325	13.00	5.66	0.04	<0.01	2
IC12-328	9.43	5.41	0.03	0.02	2
IC12-488	16.40	2.02	0.02	0.02	2
IC16-236	13.20	3.81	0.03	0.03	2
IC16-244	17.20	4.86	0.03	0.03	2

Table 1. Analytical results for samples from within or near ore deposits of Idaho Cobalt Belt--(Continued)

Field no.	Fe_2O_3* %	K_2O* %	Cl %	F %	Lithol
IC16-271	10.80	4.56	0.02	<0.01	2
IC16-281	15.10	3.46	0.02	<0.01	2
IC16-285	18.90	2.96	0.01	0.01	2
IC16-305	16.70	4.86	0.02	0.02	2
IC16-306	18.59	4.34	0.02	<0.01	2
IC16-311	12.30	2.03	---	<0.01	2
IC16-336	12.40	2.96	0.02	<0.01	2
IC16-351	20.70	2.08	0.02	<0.01	3
IC16-542	18.30	3.83	0.04	<0.01	2
IC18-700	10.30	1.76	<0.01	0.02	2
IC18-762	10.70	2.93	0.04	0.02	2
IC18-767	15.20	3.92	<0.01	<0.01	3
IC18-768	12.10	3.41	0.02	0.02	3
IC18-770	34.32	1.69	<0.01	0.02	8
IC18-781	13.40	3.08	0.02	<0.01	3
IC18-854	7.98	5.86	0.02	0.02	2
IC181064	11.20	4.39	0.02	0.01	2
IC181068	8.52	3.96	0.02	<0.01	2
IC181074	10.10	4.30	0.02	<0.01	2
IC181079	14.80	4.47	0.03	0.01	2
IC181080	8.93	4.58	0.02	0.02	2
IC181081	8.59	4.58	0.02	0.02	2
Merle deposit					
M1A-528	9.79	4.75	0.25	0.02	3
M1A-647	17.90	5.06	0.46	0.06	4
M1A-697	13.10	4.67	0.32	0.02	4
M1A-698	12.60	4.47	0.29	0.01	4
M1A-708	14.70	5.45	0.24	0.07	9
M1A-735	18.80	6.02	0.29	0.06	9
M3A-048	16.50	6.21	0.49	0.06	5
M3A-065	10.50	6.23	0.34	0.04	2
M4A-260	9.45	5.65	0.33	0.03	2
M4A-281	16.80	4.97	0.41	0.05	4
M4A-292	22.40	4.37	0.37	0.04	5
M4A-298	16.20	5.08	0.48	0.06	2
M4A-313	13.10	4.26	0.42	0.04	1
M4B-495	16.60	2.43	0.17	0.04	9
M4B-527	35.75	4.94	0.17	0.12	5
M4B-537	47.19	0.83	0.04	0.04	5
M4B-540	22.50	1.07	0.05	0.04	5
M4B-568	10.60	5.22	0.19	0.03	5
M4B-570	15.90	7.97	0.39	0.05	5
M4B-594	15.00	7.57	0.33	0.05	2

Table 1. Analytical results for samples from within or near ore deposits of Idaho Cobalt Belt--(Continued)

Field no.	Fe_2O_3* %	K_2O* %	Cl %	F %	Lithol
M5A-299	20.90	7.87	0.39	0.05	5
M5A-319	25.90	6.47	0.32	0.08	5
M5A-325	13.40	6.65	0.36	0.04	2
M5A-340	20.30	3.71	0.37	0.04	5
M5A-341	22.88	2.29	0.18	0.08	5
M5A-344	21.45	3.37	0.30	0.05	5
M5A-346	21.80	3.72	0.28	0.05	5
M5A-352	13.60	5.51	0.29	0.05	2
M5B-772	10.70	6.16	0.32	0.03	2
M5B-780	15.10	5.16	0.46	0.09	5
M5B-790	24.70	1.82	0.09	0.03	5
M5B-801	32.89	0.82	<0.01	<0.01	3
M5B-810	19.20	6.69	0.37	0.02	5
M6A-192	11.50	6.30	0.33	0.05	2
M6A-207	13.70	4.76	0.38	0.04	5
M6A-210	14.00	4.03	0.40	0.05	5
M6A-214	14.30	3.77	0.37	0.07	5
M6A-218	8.61	6.23	0.21	0.03	5
M6A-236	11.10	7.19	0.29	0.03	2
M7A-150	21.90	6.62	0.39	0.04	5
M7A-188	22.40	5.30	0.31	0.07	5
M7A-202	15.30	5.40	0.46	0.02	2
M7A-234	12.70	5.03	0.38	0.02	2
M7A-239	25.74	4.22	0.46	0.02	5
M7A-247	12.10	5.03	0.34	0.02	5
M7B-313	17.00	5.03	0.60	0.02	2
M7B-317	20.30	4.31	0.39	0.02	5
M7B-319	24.31	3.25	0.24	0.04	5
M7B-320	24.31	2.53	0.25	0.03	8
M7B-329	11.70	7.15	0.44	0.02	4
M7B-427	18.80	7.71	0.36	0.03	1
M7B-435	14.00	5.17	0.24	0.03	5
M7B-436	14.00	3.56	0.28	0.02	5
M7B-439	14.30	3.13	0.33	0.02	5
M7B-445	8.76	1.08	0.10	0.02	8
M7B-449	12.30	3.67	0.39	0.03	2
M7B-463	17.50	5.19	0.60	0.04	5
M8A-146	10.50	6.60	0.41	0.02	5
M8A-151	21.45	7.11	0.68	0.04	5
M8A-158	28.90	6.20	0.58	0.05	5
M8A-165	14.20	7.27	0.47	0.05	2
M8A-206	12.90	5.22	0.35	0.03	5
M8A-297	16.80	4.83	0.56	0.02	5
M8A-305	21.45	4.58	0.31	0.04	5

Table 1. Analytical results for samples from within or near ore deposits of Idaho Cobalt Belt--(Continued)

Field no.	Fe_2O_3* %	K_2O* %	Cl %	F %	Lithol
M8A-315	21.70	7.83	0.33	0.03	5
M8A-350	22.60	6.22	0.50	0.04	5
M9A-165	21.30	5.91	0.50	0.04	4
M9A-192	18.30	6.99	0.49	0.01	5
M9B-078	15.50	4.66	0.47	0.02	5
M9B-199	13.40	6.82	0.41	0.02	4
M9B-243	19.40	6.07	0.74	0.02	4
M9B-262	22.40	8.42	0.59	0.02	5
M9B-263	19.70	7.79	0.49	0.04	5
M9B-267	16.30	4.62	0.48	0.04	5
M10A-190	16.90	7.30	0.42	0.03	5
M10A-197	16.70	4.89	0.45	0.02	5
M10A-210	13.20	3.54	0.36	0.02	8
M10A-214	11.10	5.13	0.41	0.01	2
M10A-258	18.70	6.77	0.49	0.04	5
M10A-303	21.20	6.43	0.66	0.02	4
M10A-348	22.50	6.06	0.51	0.03	4
M10A-360	12.80	5.23	0.45	0.02	2
M10B-326	8.90	5.91	0.26	0.01	3
M10B-332	14.00	5.79	0.36	0.03	2
M10B-333	44.33	1.93	0.11	0.04	5
M10B-337	17.20	4.01	0.38	0.06	5
M10B-339	14.70	4.48	0.33	0.02	2
M10B-498	10.60	4.72	0.31	0.02	1
M10B-499	11.80	4.47	0.30	0.03	3
M10B-505	13.10	4.65	0.40	0.02	2
M11A-138	16.10	4.86	0.52	0.02	4
M11A-147	8.40	2.92	0.28	0.02	4
M11A-153	13.20	3.34	0.25	0.01	5
M11A-159	12.70	4.82	0.40	0.02	3
M11A-160	11.20	4.22	0.34	0.01	2
M11A-233	10.10	5.83	0.30	<0.01	1
M11A-234	9.79	5.88	0.31	<0.01	1
M11A-248	12.50	5.81	0.33	<0.01	1
M11A-258	22.50	7.00	0.32	<0.01	5
M11A-304	12.30	4.44	0.36	0.01	3
M11A-309	16.00	4.40	0.34	0.03	3
M11B-222	5.76	5.69	0.19	0.01	3
M11B-246	15.73	4.58	0.40	0.03	5
M11B-249	21.80	6.43	0.67	0.05	5
M11B-264	15.73	2.41	0.33	0.03	4
M11B-268	27.90	5.70	0.33	0.03	1
M11B-497	17.80	7.29	0.54	0.04	2
M11B-520	27.50	6.83	0.75	0.04	5

Table 1. Analytical results for samples from within or near ore deposits of Idaho Cobalt Belt--(Continued)

Field no.	Fe_2O_3* %	K_2O* %	Cl %	F %	Lithol
M11B-687	28.60	7.95	0.61	0.06	5
M12A-101	20.70	5.40	0.77	0.04	5
M12A-103	17.00	3.31	0.36	0.04	5
M12A-105	9.44	1.93	0.20	0.02	4
M12A-336	6.47	5.07	0.13	0.02	2
M12A-337	5.48	4.39	0.12	0.02	5
M12A-340	24.31	2.77	0.14	0.03	5
M12A-341	30.03	1.81	0.04	0.03	5
M12A-343	13.70	4.45	0.38	0.03	3
M12A-344	13.00	4.36	0.43	0.02	4
M12A-610	35.75	1.57	0.06	0.02	2
M12A-614	18.00	4.53	0.40	0.04	2
M12A-830	21.10	5.68	0.68	0.01	4
M12A-836	15.73	2.65	0.26	0.04	5
M12A-840	11.90	3.19	0.32	0.04	5
M12A-842	20.80	5.74	0.68	0.04	5
M12A-847	13.30	3.45	0.42	0.04	2
M13A-229	21.00	7.33	0.81	0.03	1
M13A-254	12.60	3.88	0.44	0.02	4
M13A-258	17.16	2.41	0.20	0.01	5
M13A-262	19.20	5.24	0.70	0.02	5
M13A-306	11.00	4.96	0.34	0.04	3
M13A-307	15.60	6.45	0.49	0.04	3
M13A-313	17.00	2.13	0.07	0.01	4
M13A-314	36.90	1.21	0.08	<0.01	5
M13A-317	31.46	1.69	0.06	<0.01	2
M13A-319	21.90	7.18	0.70	0.03	2
M13A-320	17.70	5.50	0.55	0.04	3
M13A-365	14.00	5.77	0.53	0.01	2
M13A-366	13.80	5.67	0.45	0.06	2
M14B-280	6.38	1.55	0.17	<0.01	5
M14B-340	22.20	6.13	0.73	0.06	3
M14B-348	18.59	3.98	0.49	0.03	3
M14B-352	12.10	4.97	0.35	0.01	5
M14B-356	21.45	4.58	0.46	0.04	4
M14B-358	23.20	5.48	0.61	0.06	2
Sunshine deposit					
S1A-430	11.20	4.34	0.26	0.01	2
S1A-445	19.40	3.76	0.19	0.02	2
S1A-452	20.02	3.61	0.22	<0.01	5
S1A-464	15.00	3.27	0.28	0.04	2
S1A-595	14.30	2.07	0.16	0.06	9
S2A-486	14.00	3.55	0.20	0.02	2

Table 1. Analytical results for samples from within or near ore deposits of Idaho Cobalt Belt--(Continued)

Field no.	Fe_2O_3* %	K_2O* %	Cl %	F %	Lithol
S2A-487	11.80	3.55	0.17	0.03	2
S2A-490	15.74	1.18	0.11	<0.01	4
S4A-108	16.60	2.83	0.22	0.02	2
S4A-122	18.10	2.87	0.10	0.05	5
S4A-226	11.30	4.65	0.22	0.02	2
S4A-264	12.00	4.61	0.18	0.03	5
S5A-146	9.50	4.14	0.12	0.03	2
S5A-167	30.03	6.87	0.45	0.03	5
S5A-196	20.20	4.39	0.40	0.02	2
S6A-208	12.20	2.77	0.03	0.01	2
S6A-212	18.59	1.06	0.03	<0.01	2
S6A-216	17.10	1.99	0.06	0.01	5
S6A-226	16.20	3.10	0.22	0.01	3
S6A-242	9.37	3.83	0.15	0.03	2
S7B-239	11.15	1.17	0.05	0.02	5
S7B-249	9.98	1.16	0.10	0.01	5
S7B-286	19.10	1.81	---	0.02	5
S7B-290	11.58	0.11	0.03	<0.01	5
S7B-296	21.00	2.75	0.19	0.01	2
S7B-297	21.00	2.75	0.15	0.01	2
S7B-300	15.20	2.67	0.17	0.02	5
S7B-313	14.80	4.16	0.20	0.03	2
S8A-413	8.89	0.49	0.04	<0.01	3
S8A-456	27.17	0.89	0.09	<0.01	5
S8A-473	18.40	2.53	0.13	0.02	5
S8A-474	21.10	3.58	0.24	0.02	5
S8A-475	15.50	1.92	0.01	0.01	4
S8A-476	18.80	2.51	0.16	0.02	5
S8A-490	12.20	4.22	0.16	0.02	4
S8A-500	16.40	3.96	0.18	0.02	4
S8A-502	16.50	3.53	0.16	0.03	4
S9A-077	25.30	3.51	0.32	0.03	3
S9A-146	31.46	2.17	0.16	0.02	3
S9A-191	8.88	0.05	0.02	<0.01	5
S9A-192	10.30	0.10	0.02	<0.01	1
S9A-193	8.29	<0.06	0.01	0.01	2
S9A-198	12.73	<0.06	0.01	<0.01	1
S9A-204	15.00	2.32	0.10	0.01	1
S9A-206	14.70	2.35	0.12	0.02	2
S9A-222	20.80	3.06	0.21	<0.01	4
S9A-266	19.10	3.68	0.30	0.02	4
S9A-330	14.40	5.06	0.36	0.02	2
S10A-253	11.90	4.01	0.17	0.03	3
S10A-369	24.20	1.23	0.08	0.01	9

Table 1. Analytical results for samples from within or near ore deposits of Idaho Cobalt Belt--(Continued)

Field no.	Fe_2O_3* %	K_2O* %	Cl %	F %	Lithol
S10A-382	30.03	2.77	0.21	0.03	4
S10A-438	16.40	2.06	0.17	0.03	3
S10A-487	18.10	1.40	0.11	<0.01	3
S10A-492	8.44	0.51	0.02	<0.01	5
S10A-495	6.86	0.43	0.04	<0.01	5
S10A-497	16.90	3.67	0.19	0.02	3
S10A-500	14.20	4.23	0.19	0.03	2
S10A-534	11.50	4.44	0.17	0.02	2
S10B-555	11.20	4.69	0.20	0.02	2
S10B-565	14.00	4.26	0.21	0.03	3
S10B-568	17.16	3.01	0.19	<0.01	5
S10B-577	20.02	2.29	0.12	<0.01	5
S10B-580	11.80	3.42	0.02	0.01	2
S10B-588	17.00	4.91	0.27	0.02	2
S10B-590	8.03	3.90	0.14	0.02	2
S10B-630	13.40	4.87	0.24	0.03	2
S11A-219	13.20	2.37	0.17	<0.01	5
S11A-223	9.44	1.00	0.07	<0.01	5
S11A-226	22.20	3.20	0.33	<0.01	4
S11A-229	14.60	2.99	0.18	<0.01	5
S11A-236	15.40	1.64	0.19	0.01	1
S12A-477	23.20	3.95	0.26	0.02	1
S12A-499	17.90	3.05	0.14	0.02	2
S12A-531	26.00	5.88	0.44	0.04	5
S12A-548	13.50	5.00	0.31	0.05	2
S12B-533	22.50	3.34	0.22	0.03	2
S12B-541	23.40	2.64	0.15	0.02	5
S12B-555	24.90	1.89	0.14	<0.01	5
S12B-562	11.90	4.23	0.28	0.03	2
S12B-617	27.30	6.04	0.40	0.08	9
S12C-678	9.63	4.60	0.20	0.02	2
S12C-713	25.50	2.85	0.20	<0.01	5
S12C-723	10.80	4.73	0.26	0.03	2
S13A-584	11.90	4.39	0.20	0.02	2
S13A-592	20.30	2.06	0.19	<0.01	2
S13A-596	8.82	3.92	0.17	0.03	2
S14B-710	11.60	5.29	0.27	0.03	3
S14B-742	10.70	2.48	0.07	0.02	3
S14B-744	11.50	2.52	0.04	0.01	2
S14B-746	14.30	1.13	0.05	0.01	2
S14B-747	15.40	3.49	0.12	0.01	5
S14B-750	9.77	4.49	0.15	0.03	2
S14B-764	9.64	4.53	0.20	0.02	2
S15A-499	16.90	6.16	0.26	0.03	5

Table 1. Analytical results for samples from within or near ore deposits of Idaho Cobalt Belt--(Continued)

Field no.	Fe_2O_3* %	K_2O* %	Cl %	F %	Lithol
S15A-515	10.50	5.29	0.30	0.04	2
S15A-548	19.40	7.05	0.31	0.06	9
S16A-621	15.90	4.52	0.26	0.02	5
S16A-623	30.03	5.42	0.24	0.03	5
S16A-626	31.46	4.10	0.18	0.03	5
S16A-629	11.90	3.07	0.09	0.02	2
S16A-634	12.00	5.16	0.21	0.02	2
S16B-450	24.60	7.83	0.36	0.02	5
S16B-534	32.89	5.18	0.32	0.02	5
S16B-558	17.90	2.14	0.12	0.01	5
S16B-560	21.45	0.45	--	0.06	5
S16B-564	31.46	2.05	0.10	0.04	5
S16B-566	15.00	2.32	0.13	0.01	2
S16B-573	17.10	4.68	0.19	0.02	2
S16C-412	14.20	3.77	0.15	0.02	2
S16C-442	25.20	3.90	0.30	0.03	2
S16C-448	18.10	4.39	0.26	0.04	4
S16C-455	23.40	5.46	0.35	0.04	5
S16C-498	16.20	2.98	0.16	<0.01	2
S17A-749	19.50	7.56	0.32	0.03	5
S17A-763	11.40	5.24	0.24	0.03	4
S17A-775	13.10	4.28	0.26	0.02	5
S17A-777	21.45	3.98	0.18	0.02	5
S17A-780	17.80	5.11	0.48	0.02	2
S17A-792	8.15	5.28	0.19	0.03	4
S17B-412	15.90	1.10	0.10	0.02	9
S17B-629	17.10	2.87	0.25	0.03	2
S17B-638	30.03	0.74	0.11	<0.01	5
S17B-661	19.00	3.88	0.33	0.02	5
S17B-666	20.10	3.64	0.21	0.02	5
S17B-668	19.40	2.86	0.17	0.02	5
S17B-672	37.18	3.37	0.14	0.01	5
S17B-673	17.00	4.75	0.28	0.02	5
S17B-675	15.20	4.94	0.40	0.04	2
S17B-682	11.80	4.60	0.34	0.03	2
South Idaho deposit					
SI1A-405	34.32	9.28	1.10	0.04	5
SI1B-165	16.00	6.10	0.34	0.04	5
SI3A-236	32.89	9.40	0.93	0.08	5
SI4B-125	23.70	4.63	0.18	0.05	5

Table 1. Analytical results for samples from within or near ore deposits of Idaho Cobalt Belt--(Continued)

Field no.	Fe_2O_3* %	K_2O* %	Cl %	F %	Lithol
Samples from surface exposures					
NIC500	12.80	4.55	0.14	0.06	5
NIC501	4.12	4.74	0.07	0.02	5
NIC504S	2.27	0.77	0.08	<0.01	3
NIC504T	9.37	1.72	0.09	0.07	5
NIC505	11.50	2.62	0.12	0.08	5
NIC506	16.70	8.40	0.26	0.09	5
NIC507	11.20	8.79	0.31	0.04	5
NIC508	15.60	4.62	0.19	0.04	5
NIC510	25.60	8.05	0.33	0.07	5
NIC511	19.30	5.47	0.63	0.04	5
NIC512	14.50	6.80	0.47	0.04	5
NIC514	16.00	2.55	0.16	0.02	6
NIC520	14.70	2.43	0.08	<0.01	6
NIC521	19.90	3.75	0.23	0.02	6
NIC522	12.00	1.87	0.10	<0.01	6
NIC523	23.00	4.07	0.17	0.04	6
NIC524	15.40	3.48	0.11	0.02	6
NIC525	21.60	2.25	0.08	<0.01	6
NIC526	23.30	7.50	0.52	0.04	5
NIC527A	22.00	2.19	0.20	0.02	5
NIC527C	11.10	1.51	0.14	0.02	6
NIC528	11.70	3.08	0.05	0.01	6
NIC529	12.80	3.36	0.13	0.01	6
NIC531	34.32	1.45	0.07	<0.01	6
NIC533	27.70	1.94	0.11	0.01	6
NIC534	18.10	3.06	0.24	0.02	6
NIC550	15.30	5.40	0.35	0.07	5
NIC551	7.23	4.82	0.21	0.02	5
NIC552	20.70	2.99	0.18	0.02	6
NIC553	17.50	5.30	0.24	0.10	5
NIC554	15.60	5.14	0.29	0.04	5
NIC555	22.00	6.52	0.23	0.03	6
NIC556	8.49	4.44	0.22	0.02	5
NIC557	17.00	6.19	0.44	0.02	6
NIC558	30.03	4.10	0.21	0.06	6
NIC559	12.20	2.15	0.12	0.02	6
NIC570	6.36	5.83	0.13	0.01	5
NIC571	7.95	3.32	0.31	0.03	5
NIC574	19.60	7.33	1.01	0.08	5
NIC575	3.25	3.35	0.60	0.02	5

LITHOL: 1, argillite; 2, siltite; 3, fine quartzite; 4, biotite-rich siltite; 5, biotite rock (predominantly biotite); 6, biotitie-garnet rock; 9, mafic dike or sill.

Table 2. Analytical results and descriptions of typical Yellowjacket Formation samples, Lemhi Co., Idaho

[< , less than given value; --, not analyzed]

Sample	$FeTO_3$ %	K_2O %	Cl %	F %
JC3Y01R	4.25	2.29	0.03	0.01
JC3Y01T	5.39	3.68	.01	.01
JC3Y02R	4.69	3.81	.06	.01
JC3Y02T	4.50	2.40	.01	.01
JC3Y03R	4.84	2.74	.02	.01
JC3Y03T	4.58	0.91	<.01	.01
JC3Y04R	3.70	3.76	.02	.01
JC3Y04T	6.17	3.56	.01	.03
JC3Y05R	4.00	3.54	.01	.01
JC3Y05T	6.78	3.44	.02	.01
JC3Y06R	4.51	4.80	.01	.01
JC3Y06T	16.70	2.22	<.01	.01
JC3Y07R	1.28	3.61	<.01	.01
JC3Y07T	--	--	<.01	<.01
JC3Y08R	4.15	6.47	.02	.01
JC3Y08T	4.99	3.85	.02	.03
JC3Y09R	3.10	5.18	.03	.01
JC3Y09T	4.03	2.47	<.01	.01
JC3Y10T	4.91	4.75	.03	.02
JC3Y11T	8.94	3.85	.10	.01
JC3Y12T	--	--	<.01	.01
JC3Y13T	4.24	5.79	.02	.01
JC3Y14T	11.00	8.60	.22	.03
JC3Y15T	14.40	1.64	.07	.02
JC4Y01T	4.01	3.46	.02	.05
JC4Y04T	3.59	3.98	.01	.03
JC4Y06T	--	--	<.01	.02
JC4Y07T	4.64	3.59	.01	.04
JC4Y09T	--	--	<.01	<.01
JC4Y10T	--	--	<.01	<.01
JC4Y11T	5.13	3.03	.02	.02
JC4Y15T	1.57	.86	<.01	<.01
JC4Y16T	3.33	5.00	.00	.02
JC4Y18T	4.02	5.04	.05	.05
JC4Y19T	4.07	3.99	.00	.09

Table 2. Analytical results and descriptions of typical Yellowjacket Formation samples, Lemhi Co., Idaho--(Continued)

Sample	$FeTO_3$ %	K_2O %	Cl %	F %
JC4Y22T	4.99	3.32	<.01	.03
JC4Y24T	5.54	3.16	<.01	.06
JC4Y26T	3.96	6.19	.05	.06
JC4Y28T	4.27	4.15	.02	.05
JC4Y29T	2.03	1.99	<.01	.01
JC4Y30T	3.49	2.43	.01	.03
JC4Y31T	--	--	<.01	<.01
JC4Y32T	4.87	2.91	.08	.03
JC4Y35T	1.59	.85	.01	.03
JC4Y36T	2.97	1.03	.39	.04
JC4Y37T	3.29	8.34	.01	.03
JC4Y38T	3.48	3.16	.01	.03
JC4Y43T	3.40	3.93	.09	<.01
JC4Y44T	--	--	<.01	.01
JC4Y45T	--	--	<.01	<.01
JC4Y46T	--	--	<.01	<.01
JC4Y47T	5.38	1.97	.06	.02
JC4Y49T	--	--	<.01	<.01
JC4Y52T	--	--	<.01	<.01
JC4Y53T	--	--	<.01	.03
JC4Y54T	--	--	.02	.01
JC4Y55T	--	--	<.01	.01
JC4Y56T	--	--	.04	.02
JC4Y57T	--	--	<.01	.02
JC4Y60T	4.46	8.21	.39	.06
JC4Y65T	16.90	7.08	.43	.06
JC4Y66T	11.70	4.34	.81	.07
JC4Y67T	1.75	2.54	.08	<.01
JC4Y68T	5.70	5.40	.14	.03
JC4Y69T	1.78	.55	.00	<.01
JC4Y70T	--	--	.02	.02
JC4Y73T	--	--	<.01	<.01
JC5Y01T	5.20	2.13	<.01	.01
JC5Y02T	2.90	1.32	<.01	.02
JC5Y03T	2.89	1.18	.01	.01
JC5Y04T	5.25	6.87	<.01	.08
JC5Y05T	4.03	1.85	<.01	.01

Table 2. Analytical results and descriptions of typical Yellowjacket Formation samples, Lemhi Co., Idaho--(Continued)

Sample	$FeTO_3$ %	K_2O %	Cl %	F %
JC5Y05X	4.10	1.84	<.01	.02
JC5Y06T	3.67	2.38	<.01	.03
JC5Y07T	3.69	3.17	<.01	.01
JC5Y08T	4.56	2.90	<.01	.02
JC5Y08X	4.60	2.92	<.01	.02
JC5Y09T	3.58	3.93	.02	.03
JC5Y10T	3.99	4.10	.01	.03
JC5Y10X	4.03	4.16	.02	.04
JC5Y11T	4.74	4.46	.03	.01
JC5Y12T	4.06	3.45	.02	.02
JC5Y13T	4.84	4.17	.01	.05
JC5Y14T	4.72	4.43	.01	.03
JC5Y14X	4.74	4.41	.01	.03
JC5Y15T	5.31	4.39	.03	.03
JC5Y16T	6.30	5.06	.03	.04
JC5Y17T	2.78	1.95	.02	.01
JC5Y17X	2.78	1.95	.01	.02
JC5Y18T	1.83	1.83	.01	.01
JC5Y19T	3.29	5.16	.05	.01
JC5Y21T	3.46	7.80	.04	.03
JC5Y22T	7.17	5.06	.15	.03
JC5Y22X	7.14	5.04	.15	.02
JC5Y23T	4.03	3.16	.17	<.01
JC5Y23X	4.00	3.15	.18	<.01
JC5Y24T	5.76	4.55	.15	.01
JC5Y25T	3.15	4.20	.09	.01
JC5Y26T	12.80	1.87	.19	.02
JC5Y27T	3.24	1.64	.14	<.01
JC5Y27X	3.22	1.64	.14	.01
JC5Y28T	23.90	7.68	.59	.03
JC5Y28X	23.80	7.68	.36	.04
JC5Y29T	5.03	7.29	.15	<.01
JC5Y31T	8.47	5.41	.33	.02
JC5Y31X	8.41	5.32	.25	.02
JC5Y32T	23.20	5.82	.56	.11
JC5Y33T	6.30	2.23	.29	<.01
JC5Y33X	6.30	2.25	.27	.01

Table 2. Analytical results and descriptions of typical Yellowjacket Formation samples, Lemhi Co., Idaho--(Continued)

Sample	$FeTO_3$ %	K_2O %	Cl %	F %
JC5Y34T	4.33	4.90	.02	<.01
JC5Y34X	4.29	4.87	.02	.01
JC5Y36T	3.85	6.17	.02	<.01
JC5Y36X	3.81	6.19	.03	<.01
JC5Y37T	2.20	5.25	<.01	.03
JC5Y37X	2.21	5.25	<.01	.03
JC5Y38T	5.16	6.83	.07	.01
JC5Y38X	5.18	6.74	.06	.01
JC5Y39T	2.07	1.75	.06	<.01
JC5Y39X	2.07	1.76	.07	<.01
JC5Y40T	2.04	2.97	.12	<.01
JC5Y41T	7.44	4.27	.04	<.01
JC5Y42T	6.78	4.61	.04	<.01
JC5Y42X	6.84	4.62	.03	<.01
JC5Y43T	1.63	1.40	.04	<.01
JC5Y44T	4.44	3.93	.01	.02
JC5Y45T	5.19	3.89	.03	.03
JC5Y46T	5.19	2.74	.01	.02
JC5Y46X	5.13	2.73	.01	.02
JC5Y47T	4.54	3.56	.02	.02
JC5Y48T	1.05	3.73	.02	.01
JC5Y49T	1.23	3.58	.03	.01
JC5Y49X	1.26	3.57	.03	.02
JC5Y50T	4.04	2.13	.04	.01
JC5Y50X	4.01	2.15	.05	<.01
JC5Y51T	3.84	5.62	.04	.03
JC5Y52T	4.08	2.00	<.01	.02
JC5Y53T	5.65	4.36	.01	.02
JC5Y53X	5.64	4.33	.01	.03
JC5Y54T	4.29	3.22	.02	.01
JC5Y55T	4.92	4.75	.02	.02
JC5Y56T	5.45	4.35	.01	.06
JC5Y56X	5.43	4.33	<.01	.06
JC5Y57T	4.33	3.49	.02	.03
JC5Y58T	4.65	4.68	.02	.04
JC5Y59T	3.78	4.63	.03	.03

Table 2. Analytical results and descriptions of typical Yellowjacket Formation samples, Lemhi Co., Idaho--(Continued)

Sample	$FeTO_3$ %	K_2O %	Cl %	F %
JC5Y60T	2.87	2.00	.10	.01
JC5Y61T	1.52	.09	.04	.02
JC5Y61X	1.50	.08	.04	.03
JC5Y62T	3.03	1.65	.06	.02
JC5Y62X	3.03	1.65	.05	.03
JC5Y63T	3.94	3.10	.02	.01
JC5Y64T	<.04	.06	.02	<.01
JC5Y65T	.66	1.03	.01	<.01
JC5Y66T	1.14	1.87	.04	<.01
JC5Y67T	.36	1.38	.02	<.01
JC5Y68T	4.21	5.18	.03	.03
JC5Y69T	3.08	3.45	.02	.02
JC5Y70T	3.83	6.57	.04	.03
JC5Y71T	4.47	4.34	.01	.03
JC5Y71X	4.46	4.35	.01	.02
JC5Y72T	3.82	2.60	.01	.01
JC5Y73T	3.17	4.89	.02	.04
JC5Y74T	5.39	4.93	.09	.01
JC5Y75T	2.59	4.05	.03	<.01
JC5Y76T	1.92	1.62	.01	.02

Table 2. Analytical results and descriptions of typical Yellowjacket Formation samples, Lemhi Co., Idaho--(Continued)

Sample no.	Latitude	Longitude	Name	Stratigraphic unit, and approx. geographic location
JC3Y01R	44 55 07	114 06 30	Quartzite	L. Yellowjacket, Iron Ck
JC3Y01T	44 55 07	114 04 30	Siltite	Jackass zone, Iron Ck
JC3Y02R	44 55 07	114 06 30	Quartzite	L. Yellowjacket, Iron Ck
JC3Y02T	44 57 16	114 07 08	Siltite	Jackass zone, Iron Ck
JC3Y03R	44 56 35	114 05 10	Quartzite	Jackass zone, Degan Mt
JC3Y03T	44 57 52	114 07 00	Siltite	Jackass zone, Iron Ck
JC3Y04R	44 56 43	114 04 14	Quartzite	L. Yellowjacket, Iron Ck
JC3Y04T	44 58 45	114 06 55	Siltite	M. Yellowjacket, Iron Ck
JC3Y05R	44 58 20	114 05 02	Quartzite	M. Yellowjacket, Degan Mt
JC3Y05T	44 57 13	114 06 03	Siltite	Jackass zone, Jackass Ck
JC3Y06R	44 58 32	114 05 00	Quartzite	M. Yellowjacket, Degan M
JC3Y06T	44 57 13	114 06 03	BIF	Jackass zone, Jackass Ck
JC3Y07R	44 59 45	114 04 59	Quartzite	U. Yellowjacket, Lake Mt
JC3Y07T	44 57 13	114 06 03	BIF	Jackass zone, Jackass Ck
JC3Y08R	45 00 45	114 04 59	Quartzite	U. Yellowjacket, Lake Mt
JC3Y08T	44 57 13	114 06 03	Siltite	Jackass zone, Jackass Ck
JC3Y09R	45 02 29	114 05 45	Quartzite	U. Yellowjacket, Lake Mt
JC3Y09T	44 56 45	114 03 36	Quartzite	M. Yellowjacket, Degan Mt
JC3Y10T	45 00 15	114 05 00	Diamictite	U. Yellowjacket, Lake Mt
JC3Y11T	45 07 00	114 08 00	Quartzite	U. Yellowjacket, Moccasin Ck
JC3Y12T	45 07 08	114 09 57	Tourm. bx	U. Yellowjacket, Deep Ck
JC3Y13T	45 07 04	114 10 45	Aplite sill	do.
JC3Y14T	45 06 45	114 09 37	Biotitite	do.
JC3Y15T	45 05 55	114 09 23	Mafic dike	do.
JC4Y01T	45 02 15	114 13 00	Argillite	M. Yellowjacket, Copper Ck
JC4Y04T	45 04 25	114 10 45	Argillite	M. Yellowjacket, Deep Ck
JC4Y06T	45 05 32	114 10 29	Tourm. bx	U. Yellowjacket, Deep Ck
JC4Y07T	45 03 15	114 11 58	Argillite	M. Yellowjacket, Fawn Ck
JC4Y09T	45 04 04	114 11 03	Tourm. bx	M. Yellowjacket, Deep Ck
JC4Y10T	45 04 50	114 11 30	Tourm. bx	M. Yellowjacket, Spring Ck
JC4Y11T	45 03 14	114 12 55	Argillite	M. Yellowjacket, Fawn Ck
JC4Y15T	45 02 12	114 14 10	Quartzite	M. Yellowjacket, Copper Ck
JC4Y16T	45 02 12	114 14 10	Argillite	do.
JC4Y18T	44 57 50	114 16 20	Siltite	L. Yellowjacket, Moyer Ck
JC4Y19T	45 01 25	114 18 40	Argillite	Jackass zone, Moyer Ck

Table 2. Analytical results and descriptions of typical Yellowjacket Formation samples, Lemhi Co., Idaho--(Continued)

Sample no.	Latitude approx.	Longitude	Name	Stratigraphic unit, and approx. geographic location
JC4Y22T	45 01 02	114 18 55	Argillite	Jackass zone, Panther Ck
JC4Y24T	44 55 55	114 05 42	Siltite	Jackass zone, Iron Ck
JC4Y26T	44 58 01	114 16 00	Argillite	L. Yellowjacket, Moyer Ck
JC4Y28T	45 01 55	114 17 33	Argillite	M. Yellowjacket, Panther Ck
JC4Y29T	45 00 35	114 14 40	Siltite	L. Yellowjacket, Woodtick Ck
JC4Y30T	45 02 58	114 15 15	Siltite	M. Yellowjacket, Copper Ck
JC4Y31T	45 05 35	114 12 30	Tourm. bx	U. Yellowjacket, Panther Ck
JC4Y32T	45 05 20	114 12 45	Siltite	Blackbird zone, Panther Ck
JC4Y35T	45 03 03	114 43 15	Quartzite	Yellowjacket?, Salmon R
JC4Y36T	45 02 13	114 43 30	Quartzite	do.
JC4Y37T	45 02 55	114 43 20	Quartzite	do.
JC4Y38T	45 03 58	114 43 30	Siltite	do.
JC4Y43T	45 03 10	114 07 00	Quartzite	Blackbird zone, Deep Ck
JC4Y44T	45 03 10	114 07 00	Tourm. bx	do.
JC4Y45T	45 06 00	114 14 27	Tourm. bx	Blackbird zone, Panther Ck
JC4Y46T	45 05 15	114 15 16	Tourm. bx	do.
JC4Y47T	45 05 16	114 14 30	Siltite	do.
JC4Y49T	45 06 15	114 12 15	Tourm. bx	do.
JC4Y52T	45 02 15	114 04 50	Tourm. bx	Blackbird zone, Lake Mt
JC4Y53T	45 01 50	114 04 35	Tourm. bx	do.
JC4Y54T	45 06 20	114 08 50	Tourm. bx	U. Yellowjacket, Deep Ck
JC4Y55T	45 05 55	114 08 50	Tourm. bx	do.
JC4Y56T	45 05 00	114 07 55	Tourm. bx	Blackbird zone, Deep Ck
JC4Y57T	45 06 05	114 11 10	Tourm. bx	do.
JC4Y60T	44 57 15	114 16 52	Argillite	L. Yellowjacket, Moyer Ck
JC4Y65T	45 06 32	114 10 38	Biotitite	Blackbird zone, Deep Ck
JC4Y66T	45 06 32	114 10 38	Biotitite	do.
JC4Y67T	45 06 32	114 10 38	Quartzite	do.
JC4Y68T	45 06 32	114 10 38	Argillite	do.
JC4Y69T	45 05 55	114 09 23	Quartzite	do.
JC4Y70T	45 06 37	114 10 10	Tourm. bx	do.
JC4Y73T	45 04 35	114 06 40	Tourm. bx	do.
JC5Y01T	44 57 35	114 11 42	Siltite	L. Yellowjacket, Moyer Pk
JC5Y02T	44 57 30	114 11 42	Siltite	do.
JC5Y03T	44 57 14	114 11 42	Siltite	do.

Table 2. Analytical results and descriptions of typical Yellowjacket Formation samples, Lemhi Co., Idaho--(Continued)

Sample no.	Latitude	Longitude	Name	Stratigraphic unit, and approx. geographic location
JC5Y04T	44 57 18	114 11 45	Argillite	do.
JC5Y05T	44 57 18	114 11 45	Siltite	do.
JC5Y05X	44 57 18	114 11 45	Siltite	do.
JC5Y06T	44 57 22	114 11 48	Argillite	do.
JC5Y07T	44 58 02	114 12 20	Argillite	do.
JC5Y08T	44 58 04	114 12 20	Siltite	do.
JC5Y08X	44 58 04	114 12 20	Siltite	do.
JC5Y09T	45 02 00	114 15 00	Argillite	M. Yellowjacket, Woodtick Ck
JC5Y10T	45 02 30	114 13 30	Argillite	M. Yellowjacket, Copper Ck
JC5Y10X	45 02 30	114 13 30	Argillite	do.
JC5Y11T	45 02 30	114 13 30	Argillite	M. Yellowjacket, Copper Ck
JC5Y12T	45 03 00	114 13 00	Argillite	do.
JC5Y13T	45 03 30	114 12 00	Argillite	M. Yellowjacket, Deep Ck
JC5Y14T	45 03 00	114 12 00	Argillite	do.
JC5Y14X	45 03 00	114 12 00	Argillite	do.
JC5Y15T	45 04 30	114 11 00	Argillite	M. Yellowjacket, Spring Ck
JC5Y16T	45 04 00	114 11 00	Argillite	M. Yellowjacket, Deep Ck
JC5Y17T	45 04 00	114 09 30	Siltite	do.
JC5Y17X	45 04 00	114 09 30	Siltite	do.
JC5Y18T	45 04 00	114 09 30	Quartzite	do.
JC5Y19T	45 05 00	114 09 30	Quartzite	do.
JC5Y21T	45 06 32	114 10 38	Argillite	Blackbird zone, Deep Ck
JC5Y22T	45 06 32	114 10 38	Biotitite	do.
JC5Y22X	45 06 32	114 10 38	Biotitite	do.
JC5Y23T	45 05 55	114 09 23	Quartzite	do.
JC5Y23X	45 05 55	114 09 23	Quartzite	do.
JC5Y24T	45 05 55	114 09 23	Argillite	do.
JC5Y25T	45 06 37	114 09 40	Argillite	do.
JC5Y26T	45 06 37	114 09 40	Mafic sill?	do.
JC5Y27T	45 06 37	114 09 40	Quartzite	do.
JC5Y27X	45 06 37	114 09 40	Quartzite	do.
JC5Y28T	45 06 45	114 09 37	Biotitite	do.
JC5Y28X	45 06 45	114 09 37	Biotitite	do.
JC5Y29T	45 06 30	114 10 00	Argillite	do.
JC5Y31T	45 07 00	114 11 00	Argillite	do.

Table 2. Analytical results and descriptions of typical Yellowjacket Formation samples, Lemhi Co., Idaho--(Continued)

Sample no.	Latitude	Longitude	Name	Stratigraphic unit, and approx. geographic location
JC5Y31X	45 07 00	114 11 00	Argillite	do.
JC5Y32T	45 07 00	114 11 00	Biotitite	do.
JC5Y33T	45 07 13	114 10 30	Quartzite	U. Yellowjacket, Deep Ck
JC5Y33X	45 07 13	114 10 30	Quartzite	do.
JC5Y34T	45 00 38	114 05 45	Quartzite	U. Yellowjacket, Lake Mt
JC5Y34X	45 00 38	114 05 45	Quartzite	do.
JC5Y36T	45 00 50	114 05 00	Quartzite	do.
JC5Y36X	45 00 50	114 05 00	Quartzite	do.
JC5Y37T	45 01 20	114 05 07	Quartzite	do.
JC5Y37X	45 01 20	114 05 07	Quartzite	do.
JC5Y38T	45 02 16	114 05 43	Quartzite	do.
JC5Y38X	45 02 16	114 05 43	Quartzite	do.
JC5Y39T	45 03 25	114 04 40	Quartzite	U. Yellowjacket, Williams Ck
JC5Y39X	45 03 25	114 04 40	Quartzite	do.
JC5Y40T	45 06 50	114 07 08	Quartzite	U. Yellowjacket, Moccasin Ck
JC5Y41T	45 08 52	114 00 55	Quartzite	U. Yellowjacket, Baldy Mt
JC5Y42T	45 09 33	114 01 32	Quartzite	U. Yellowjacket, Pollard Ck
JC5Y42X	45 09 33	114 01 32	Quartzite	do.
JC5Y43T	45 12 02	114 02 33	Quartzite	U. Yellowjacket, Turner Ck
JC5Y44T	45 00 25	114 11 15	Argillite	L. Yellowjacket, Woodtick Ck
JC5Y45T	45 00 20	114 11 30	Argillite	do.
JC5Y46T	44 58 20	114 11 35	Argillite	Jackass zone, Moyer Pk
JC5Y46X	44 58 20	114 11 35	Argillite	do.
JC5Y47T	44 58 40	114 11 39	Argillite	do.
JC5Y48T	44 55 12	114 06 45	Quartzite	L. Yellowjacket, Iron Ck
JC5Y49T	44 55 12	114 06 45	Quartzite	do.
JC5Y49X	44 55 12	114 06 45	Quartzite	do.
JC5Y50T	44 55 12	114 06 40	Quartzite	do.
JC5Y50X	44 55 12	114 06 40	Quartzite	do.
JC5Y51T	44 55 20	114 06 43	Argillite	do.
JC5Y52T	44 56 25	114 07 05	Siltite	do.
JC5Y53T	44 56 47	114 07 14	Argillite	do.
JC5Y53X	44 56 47	114 07 14	Argillite	do.
JC5Y54T	44 57 13	114 07 13	Siltite	do.
JC5Y55T	45 03 18	114 24 17	Argillite	Jackass zone, Porphyry Ck

Table 2. Analytical results and descriptions of typical Yellowjacket Formation samples, Lemhi Co., Idaho--(Continued)

Sample no.	Latitude	Longitude	Name	Stratigraphic unit, and approx. geographic location
JC5Y56T	45 03 15	114 24 32	Siltite	do.
JC5Y56X	45 03 15	114 24 32	Siltite	do.
JC5Y57T	45 03 05	114 24 47	Argillite	do.
JC5Y58T	45 02 02	114 23 18	Argillite	do.
JC5Y59T	45 02 02	114 23 01	Argillite	do.
JC5Y60T	44 58 52	114 31 46	Siltite	L. Yellowjacket, Yellowj. Ck
JC5Y61T	44 58 38	114 31 08	Quartzite	do.
JC5Y61X	44 58 38	114 31 08	Quartzite	do.
JC5Y62T	44 58 35	114 30 15	Siltite	do.
JC5Y62X	44 58 33	114 30 15	Siltite	do.
JC5Y63T	44 59 08	114 29 45	Siltite	do.
JC5Y64T	44 59 30	114 29 14	Quartzite	Hoodoo, Yellowjacket Ck
JC5Y65T	44 59 42	114 28 55	Quartzite	do.
JC5Y66T	45 00 06	114 28 37	Quartzite	Hoodoo, Shovel Ck
JC5Y67T	45 00 20	114 27 50	Quartzite	do.
JC5Y68T	45 00 25	114 27 38	Argillite	L. Yellowjacket, Shovel Ck
JC5Y69T	45 01 28	114 26 47	Argillite	do.
JC5Y70T	45 01 50	114 26 43	Argillite	do.
JC5Y71T	45 02 20	114 17 50	Siltite	M. Yellowjacket, Panther Ck
JC5Y71X	45 02 20	114 17 50	Siltite	do.
JC5Y72T	45 02 36	114 17 20	Argillite	M. Yellowjacket, Panther Ck
JC5Y73T	45 03 02	114 16 47	Argillite	do.
JC5Y74T	45 04 45	114 15 37	Quartzite	do.
JC5Y75T	45 06 30	114 13 00	Quartzite	Blackbird zone, Panther Ck
JC5Y76T	44 51 05	113 58 36	Quartzite	Yellowjacket?, Salmon R

LIST OF FIGURES AND TABLES